Tanzania Journal of Science 49(3): 629-641, 2023
ISSN 0856-1761, e-ISSN 2507-7961

Optical Characterization of Photocatalytic Tungsten Oxide/Tin Oxide (WO_3/SnO_2) Thin Films for Use in Degradation of Water Pollutants

Victor Isahi[1*], Christopher Maghanga[1], Mghendi Mwamburi[2], Onesmus Munyati[3], Sylvester Hatwaambo[4], Emmanuel Akoto[1], Wycliffe Isoe[5] and Mir Waqas Alam[6]

[1]*Department of Biological & Physical Sciences, Kabarak University, P.O. Box Private Bag, 20157, Kabarak, Kenya.*

[2]*Department of Physics, University of Eldoret, P.O. Box 1125 - 30100, Eldoret, Kenya.*

[3]*Departmet of Chemistry, University of Zambia, P.O. Box 32379, Lusaka, Zambia.*

[4]*Department of Physics, University of Zambia, P.O. Box 32379, Lusaka, Zambia.*

[5]*Department of Physics, Masinde Muliro University, P.O. Box 190 -50100, Kakamega, Kenya.*

[6]*Department of Physics, College of Science, King Faisal University, P.O. Box 400, Al-Ahsa 31982, Saudi Arabia.*

**Corresponding author, email: visahi@kabarak.ac.ke*

Received 20 Jul 2023, Revised 11 Sep 2023, Accepted 15 Sep 2023 Published Sep 2023

DOI: https://dx.doi.org/10.4314/tjs.v49i3.7

Abstract

Organic pollutants in water have been a challenge and pose significant risks to human health. As a result, research efforts to eliminate these pollutants have been on the rise. Photocatalysis has shown incredible potential in water treatment containing organic pollutants since it is affordable and utilizes solar energy. Tin oxide (SnO_2) has ardently been investigated as a photocatalyst for water treatment due to its remarkable properties such as; non-toxicity, and stability. However, its wide band gap and the tendency for some electrons and holes to recombine during its use have been cited to be among limiting factors affecting its effectiveness. This study, therefore, aimed to optimize SnO_2 thin films by doping it with varied proportions of Tungsten oxide (WO_3) using Sol-gel technique and investigating the effects of WO_3 doping on the optical and photocatalytic properties of the prepared films. From the results, the calculated rate constants for SnO_2 and WO_3/SnO_2(1.5%wt.) were 0.00256 min^{-1} and 0.00519 min^{-1}, respectively, and the corresponding band gaps were 3.82 and 3.03 eV, suggesting that doping improved the optical absorbance of the films and caused a red shift of the absorption edge of the films. These results show WO_3/SnO_2 is a good candidate for photocatalytic water treatment.

Keywords: Doping, sol-gel, photocatalysis, optical characterization, WO_3/SnO_2

Introduction

Globally, one in three individuals living today do not have adequate access to safe drinking water (United Nations 2022). A World Health Organization (WHO) report indicates that contaminated drinking water can transmit diseases such as diarrhea, cholera, dysentery, typhoid, and polio, which cause many deaths annually (Buchholz 2022, World Heath Organization 2022). Organic substances are one of the major pollutants in contaminated water that are as a result of substances such as toxic dye effluents discharged from various industries which contaminate rivers and other water resources (Manikandan et al. 2018, Ojha and Tiwary 2021). Therefore, research related to finding affordable, effective, and healthy approaches to eliminate these toxic dyes has been on the rise in recent years. Among various

decontamination techniques, photocatalysis has shown immense potential due to its simplicity, low cost, non-toxicity, eco-friendliness, complete degradation of pollutants, and the ability to use abundant solar energy (Ali et al. 2017, Zhu and Zhou 2019). Metal oxide photocatalysts such as TiO_2, ZnO and SnO_2 have shown promising performance in the removal of organic pollutants (Chatterjee and Dasgupta 2005, Han et al. 2014, Iqbal et al. 2018). However, wide-bandgap and high electron-hole pair recombination affect their photocatalytic efficiency (Ishchenko et al. 2021), thus preventing extensive and practical use in photocatalytic applications (Ameta and Sharma 2015). Studies suggest that doping significantly improves the optical and photocatalytic properties of SnO_2 (Table 1). Specifically, dopants, such as Ag^+, WO_3, and W have previously been reported to improve the photocatalytic execution properties of oxide catalysts particularly TiO_2 (Behnajady et al. 2006, Ramos-Delgado et al. 2013, Wang et al. 2016). In the presence of radiation, the dopants act as electron-accepting species, thereby improving photocatalytic activity (Wang et al. 2016). It follows therefore that WO_3 as a dopant can serve to decrease the recombination rate of SnO_2 photocatalyst hence improving its photocatalytic properties. Although much research has been done on WO_3 and SnO_2, there is limited information on the combination of these two materials through doping for photocatalytic water treatment applications. Some of the works based on SnO_2 are presented in Table 1.

Table 1: Summary of some selected works on doped SnO_2 thin films for photocatalytic studies

Reference	Title of study	Key findings
Manikandan et al. (2018)	Ag activated SnO_2 films for enhanced photocatalytic dye degradation against toxic organic dyes	Doping decreased the bang gap of pure SnO_2 from 3.5eV and 3.2 eV. SnO_2:Ag film exhibits better photocatalytic activity compared to SnO_2
Raj et al. (2020)	Study on the synergistic effect of terbium-doped SnO_2 thin film photocatalysts for dye degradation	Doping tin(IV) oxide (SnO_2) with Tb increased SnO_2's absorbance, and decreased its band gap values providing more photon absorption which enhanced the photocatalytic reaction improving the rate constant
Zarei et al. (2022)	Photocatalytic properties of ZnO/SnO_2 nanocomposite films: role of morphology	The ZnO/SnO_2 film had higher photodegradation rate of methylene blue dye under ultraviolet irradiation, than that of the pristine ZnO and SnO_2 films due to the effective separation of hole–electron pairs
Azim et al. (2021)	$GO-SnO_2$ Nanocomposite for photodegradation of methyl orange under direct sunlight irradiation and mechanism	wide band gap of SnO_2 was tuned using GO which showed enhanced photocatalytic performance with greater effective surface area compared to pure SnO_2
Doyan et al. (2019)	The effect of indium doped SnO_2 thin films on optical properties prepared by Sol-Gel Spin Coating Technique	SnO_2 thin films underwent a drop in band gap from 3.64 to 3.57 eV with increase in doping.

The WO_3/SnO_2 thin film synthesis can be achieved using several techniques including Sol-gel, Chemical Bath Deposition, Spray Pyrolysis, Electroplating, Electroless Deposition, Chemical Vapour Deposition, Evaporation, and Sputtering (Jilani et al., 2017). However, in this study Sol-gel was preferred because it is a simple, fast, and low

cost technique, that has several advantages such as controlled stoichiometry, better homogeneity, low processing temperature, high purity, effective control of properties such as film thickness, and the ability to easily scale up (Chaudhary 2021, Huang et al. 2021, Parashar et al. 2020, Tseng et al. 2010).

Materials and Methods

Preparation of SnO_2 and WO_3/SnO_2 thin films

The materials used were sodium tungsten dihydrate ($Na_2WO_4.2H_2O$, 99% Merck), nitric (V) acid (HNO_3, 65% Merck), hydrogen peroxide (H_2O_2, 30% Merck), tin(II) chloride dihydrate ($SnCl_2.2H_2O$ purified from Merck), ethanol (99.9%), methylene blue powder, distilled water, acetone and Helmanex(III) solution.

Pure SnO_2 and WO_3/SnO_2 thin films were prepared using Sol-gel spin coating technique (Marikkannan et al. 2015, Naseri et al. 2010). In a typical synthesis to prepare WO_3 precursor sol solution, 6 g of sodium tungsten dihydrate ($Na_2WO_4.2H_2O$) was immersed in 30 ml of nitric acid solution (HNO_3) for 45 minutes. After three washes with distilled water, the obtained yellow-greenish precipitate (H_2WO_4) was dissolved in 10 ml of hydrogen peroxide (to aid oxidizing H_2WO_4 to WO_3), and 1 ml of ethanol was added to the solution. After 24 hours, it was exposed to light for 2 hours using a commercial 105 W lamp to concentrate the solution. The solution's colour changed from colourless to light yellow, and it was stable for a long time. It was then left for 24 h aging. SnO_2 Precursor Sol solution was prepared by dissolving 0.5 mole of tin(II) chloride dihydrate ($SnCl_2.2H_2O$) in ethanol. The prepared solution was magnetically stirred for 5 hours in a closed conical flask and aged for 24 hours at room temperature to increase its viscosity. The prepared SnO_2 sol was mixed with controlled amounts of WO_3 sol under magnetic stirring for 2 hours to produce six groups of WO_3/SnO_2 (WO_3 of 0.0, 0.1, 0.3, 0.5, 1.5, 2.0 wt.%). Before deposition, the glass substrates were cleaned thoroughly with liquid soap, acetone, and Helmanex(III) solution using an ultrasonic cleaner to remove organic particles that might be found on the surface of the glass substrates. Finally, they were rinsed with distilled water and dried. The as-prepared sol solutions were spin-coated for 30 seconds at 1200 rpm on a glass substrate. After spin coating, the coated glass substrates were dried at 100 ºC for 10 minutes to remove any remaining organic solvent. Finally, the prepared thin films were annealed for one hour at 500 ºC in a Carborlite 301 heating furnace.

Optical characterization

The optical properties of the undoped SnO_2 and WO_3/SnO_2 (WO_3 of 0.1, 0.3, 0.5, 1.5, 2.0 w.t %) thin films were investigated using UV-VIS spectroscopy (Shimandzu UV-VIS 2600) in the wavelength range 200 to 900 nm. This rage is used because it covers the wavelength spectrum relevant to SnO_2's wide-band gap nature and absorption edge, all of which are important in driving photocatalytic reactions.

Further optical properties were modelled using SCOUT software (Theiss 2002) where the obtained experimental spectra were fitted to the simulated spectra. The software is a package of a variety of models. The choice of the model to be used in fitting of the spectra depends on the material being studied and the range of the spectrum being used. The models used in this work were Drude, Kim, Tauc-Lorentz, the harmonic and OJL interband transition model.

Evaluation of photocatalytic activity

The photocatalytic execution of the prepared samples of pure SnO_2 and WO_3/SnO_2 films was investigated using the methylene blue dye degradation test under UV light radiation using a system composed of a cabinet with a UV lamp and a magnetic stirrer as shown in Figure 1. The sample was first dipped in 80 ml of methylene blue dye solution (3 ppm) in a glass beaker and put in the dark for 60 minutes to attain the adsorption-desorption balance, the contents were then moved into a cabinet containing a UV lamp and illuminated for 120 minutes at ambient temperature. Illumination was done

at 120 minutes at ambient to minimize variations caused by potential changes in light intensity and other environmental factors like temperature over longer periods of time. To achieve a constant light intensity on the film's surface, the distance between the light source and the film was kept constant. During the photodegradation process, a dye sample of 2 ml was taken from the reacting solution every 30 minutes for absorption studies. Absorbance was measured using the UV-VIS spectrophotometer and a graph was plotted. The rate of degradation was then evaluated by comparing the methylene blue degradation of pure SnO_2, and WO_3/SnO_2 (1.5%).

The pseudo-first-order kinetic model according to Gajbhiye (2012) was used to quantify the photocatalytic activity of the samples by finding the kinetic rate constant k_c (min^{-1}); According to this model the kinetic rate constant k_c (min^{-1}) is determined by using the relation;

$$ln\left(\frac{C_t}{C_o}\right) = -k_c t \qquad (1)$$

Where; C_t is the sample concentration after degradation time t, C_o is the initial concentration of methylene blue and k_c is the rate constant.

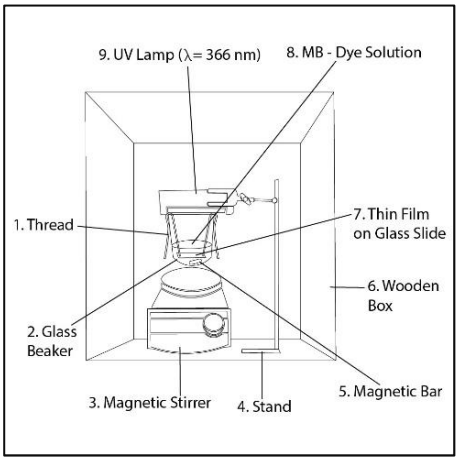

Figure 1: The experimental set-up that was used for the photocatalytic experiment.

Results and Discussion

The films had an average thickness of 135.4 nm as simulated from SCOUT software. See Figure 2.

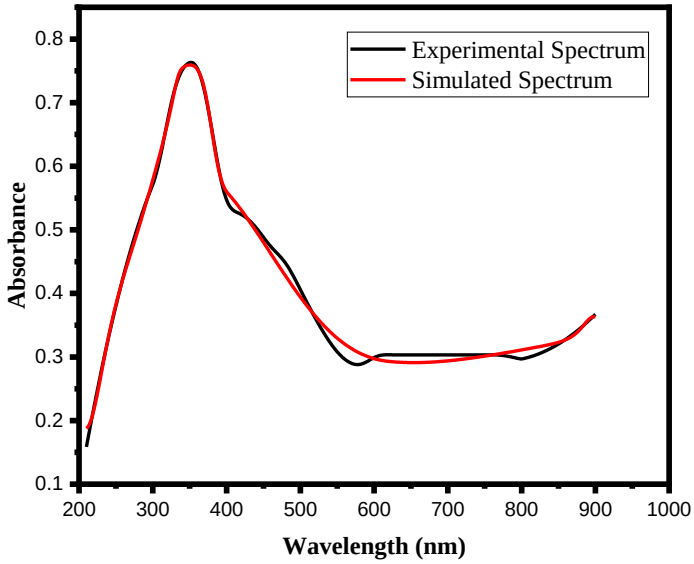

Figure 2: An illustration of fitting of the experimental to simulated spectra using the SCOUT software.

Absorbance

Figure 3 shows, the maximum absorbance of the undoped SnO_2 thin films is in the region (275 nm ≤ λ ≤ 350 nm), which is consistent with the results reported for pure SnO_2 thin films deposited by Bhagwat et al.

(2015) and Doyan et al. (2019). As observed from the spectra, there is an increase in absorbance after doping the material. This increase is due to the incorporation of WO_3 into SnO_2 which results in increased surface roughness, causing diffuse reflection and thus an increase in absorbance. It should be noted that the absorption ability of photocatalytic materials plays an important role in removal effects of pollutants (Yang et al. 2016). Greater absorption indicates a higher ability for the degradation of pollutants (Islam and Kumer 2020), implying an improvement in the photocatalytic efficiency of the films (Chen et al. 2020). WO_3/SnO_2 (1.5 wt.%) exhibits the highest optical absorbance with a wider absorption range in the visible region. Doping beyond 1.5 wt.% instead lowers the absorbance of the films. The figure also shows that the position of the absorption edge of the WO_3/SnO_2 thin film shifts towards the higher wavelength side. This red shift indicates a decrease in the band gap size (Manikandan et al. 2018).

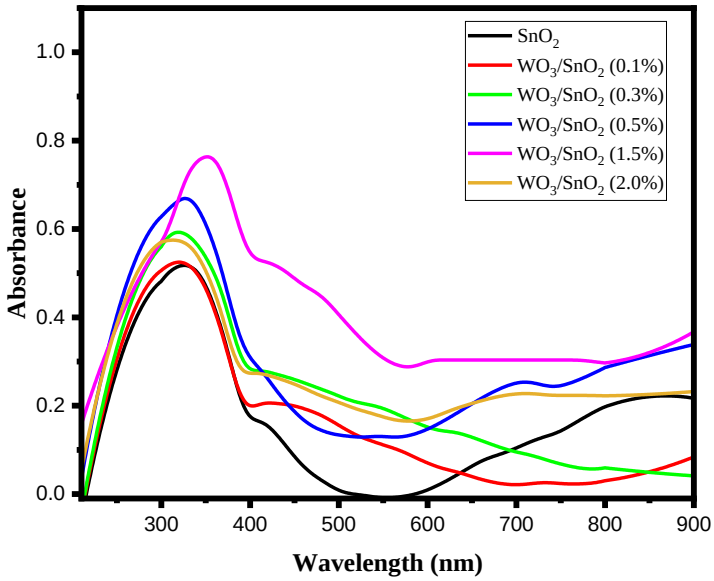

Figure 3: Absorbance as a function of wavelength for pure SnO_2 and WO_3/SnO_2 thin films with different proportions of WO_3.

Optical band gap

The excitation of an electron from the valence band to the conduction band by absorption of photon energy depends on the band gap of the material. The optical band gap E_g was calculated using Tauc's relation (Sönmezoğlu et al. 2011)

$$\alpha h\nu = A(h\nu - E_g)^n \qquad (2)$$

where α is the absorption coefficient, ν is the photon energy, and A is a constant relation between the absorption coefficient (α), and photon energy (hν). Since SnO_2 is a direct band gap material $n = {}^1/_2$, plots of $(\alpha h\nu)^2$ against hν of pure SnO_2 and WO_3/SnO_2 thin films were made, giving curves with linear parts. Extrapolation of the linear region to the hν axis was done, and the intercepts give the band gaps (E_g) of each film. Figure 4 shows the plot of $(\alpha h\nu)^2$ against hν for WO_3/SnO_2 thin films doped at varied WO_3 proportions. The extracted band gap data is presented in Table 2.

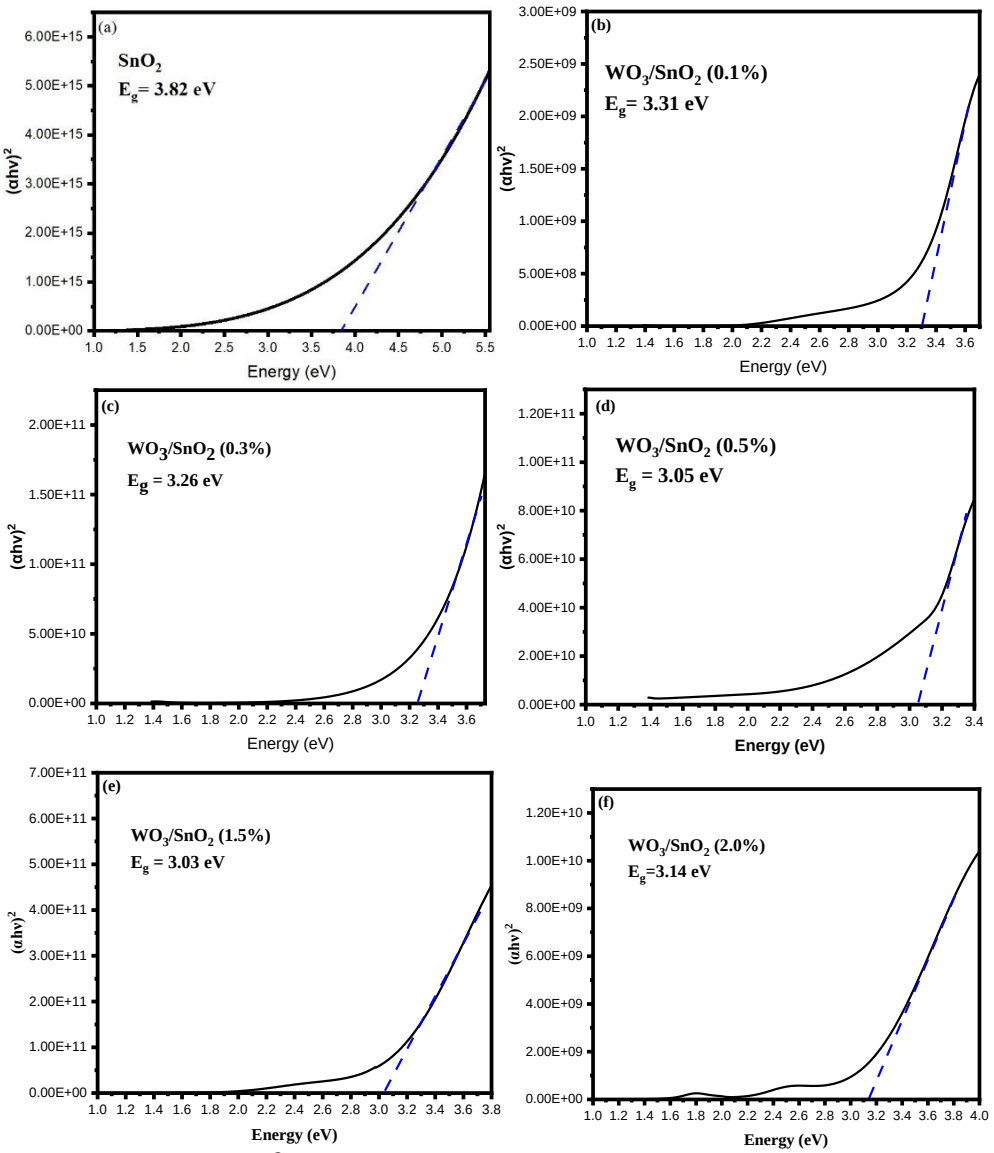

Figure 4: Plots of $(\alpha h\upsilon)^2$ versus photon energy ($h\upsilon$) for (a) pure SnO_2, (b) WO_3/SnO_2 (0.1%) (c)WO_3/SnO_2 (0.3%), (d) WO_3/SnO_2 (0.5%) (e) WO_3/SnO_2 (1.5%) and (f) WO_3/SnO_2 (2.0%) thin films.

Table 2: Summary of calculated band gap values for WO_3/SnO_2 thin films

Materials	**Band gap (eV)**
SnO_2	3.82
WO_3/SnO_2 (0.1%)	3.31
WO_3/SnO_2 (0.3%)	3.26
WO_3/SnO_2 (0.5%)	3.05
WO_3/SnO_2 (1.5%)	3.03
WO_3/SnO_2 (2.0%)	3.14

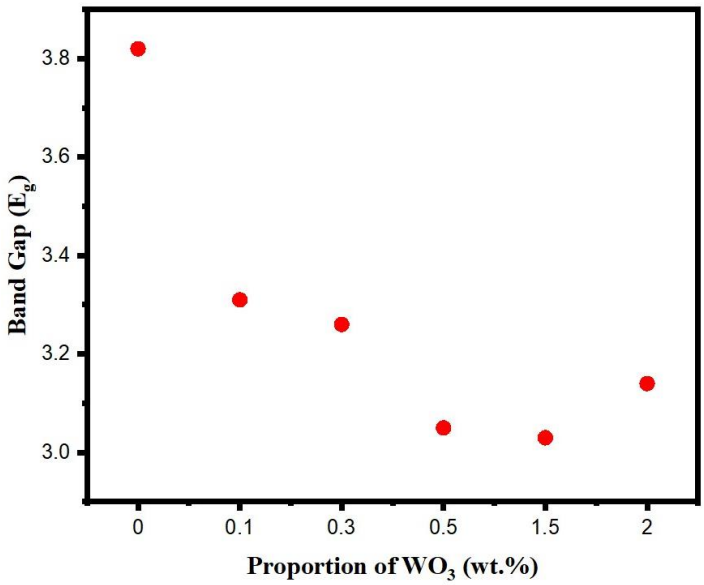

Figure 5: Change in band gap (E_g) with doping proportions of WO_3.

The band gap of undoped SnO_2 is consistent with previous work done by Bhagwat et al. (2015) and Varghese et al. (2018). From Figure 5 it can be seen that as WO_3 was introduced into SnO_2 in various doping proportions, a gradual decrease was observed in the band gap; however, beyond 1.5 %wt. doping, it began to increase. This decrease is associated with the red shift observed in the absorbance spectra, which is due to the incorporation of WO_3 into the SnO_2 lattice, which resulted in defects that narrowed the band gap (Ishchenko et al. 2021) while the increase beyond 1.5 %wt. doping is associated to the blue shift observed in the absorbance spectra. This reduction in the band gap is a key factor for the enhancement of photocatalytic activity (Koohestani 2019), because more electrons are able to gain kinetic energy and move to the conduction band, where they participate in the degradation process.

Extinction coefficient (*k*)

The extinction coefficient is a property which determines the extent to which a species absorbs or reflects light or radiation at a specific wavelength (Ubi et al. 2022). It is usually used to represent the magnitude of total amount of photons attenuated whenever the electromagnetic waves travel into the target material (Rathanasamy et al. 2023). From Figure 6, it is observed that an increase in wavelength leads to a decline in the extinction coefficient. The extinction coefficient, however, increases with dopant concentration and was found to be highest for the WO_3/SnO_2 (1.5%) sample, resulting in lesser scattering of light (Rathanasamy et al. 2023), leading to higher absorbance.

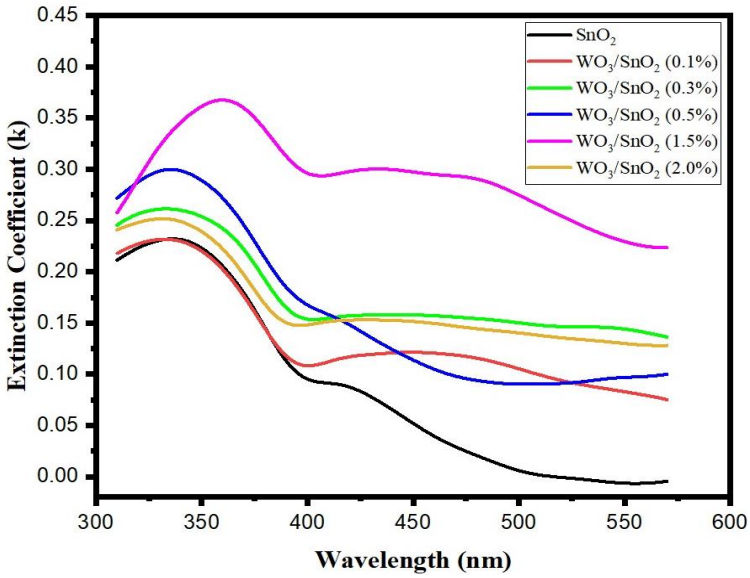

Figure 6: Extinction coefficient (k) as a function of wavelength for pure SnO_2 and WO_3/SnO_2 thin films with different proportions of WO_3.

Photocatalysis studies

Based on the optical properties, it is clear that the WO_3/SnO_2 (1.5 wt.%) thin film has superior optical properties for photocatalytic applications than all other samples. The photocatalytic properties of pure SnO_2 and WO_3/SnO_2 (1.5 wt,%) thin films were investigated using methylene blue dye under UV light. A calibration curve was made using standard methylene blue solution to calculate the concentration from measured absorbance, as shown in the Figure 7. To obtain the calibration curve, the absorbance of each standard solution was measured using a UV-VIS spectrophotometer, then a plot of the absorbance values against their known concentrations was made.

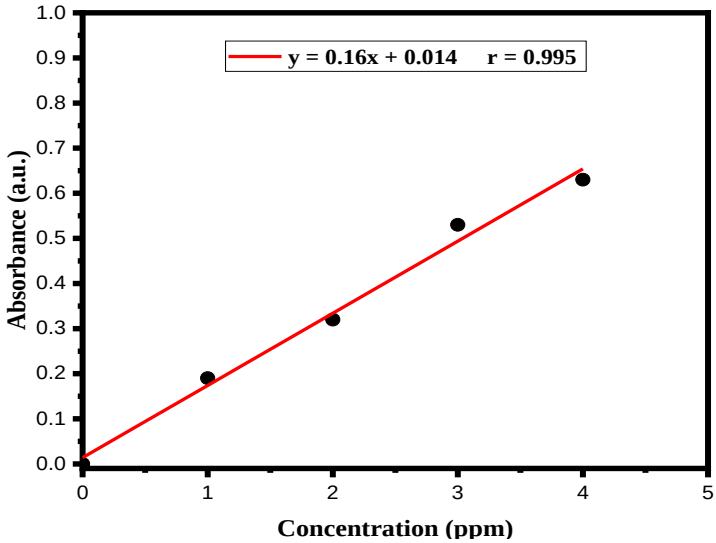

Figure 7: Methylene blue calibration curve.

In the photocatalytic experiment, fading of methylene blue solution was observed during the experiment, implying that degradation was taking place, hence an effect in its concentration. The main absorption peak located at 664 nm corresponding to MB molecules. Figure 8 shows that the absorption peak decreases with increasing exposure time, indicating that the concentration of dye molecules in the aqueous solution decreases with increasing irradiation time.

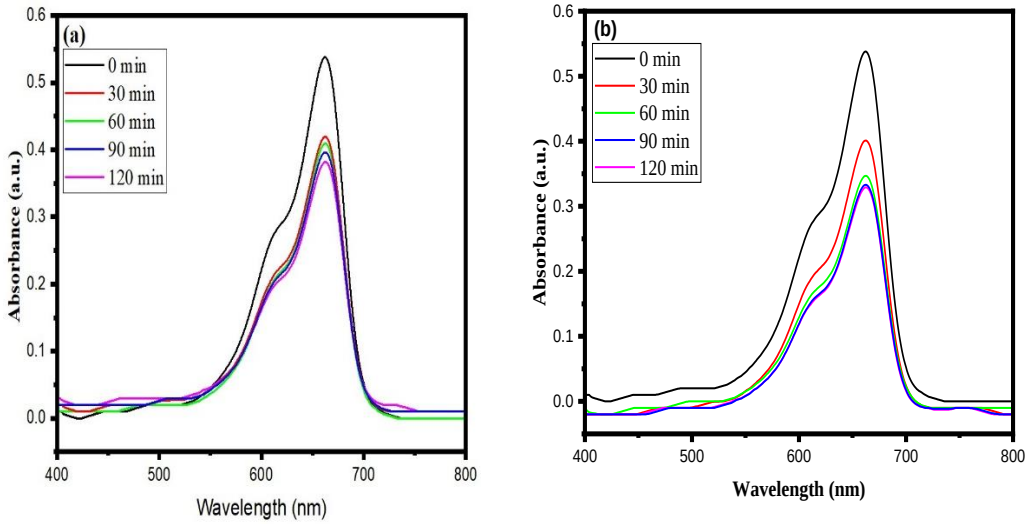

Figure 8: Absorption spectra of methylene blue for (a) SnO_2 and (b) WO_3/SnO_2 (1.5%) films.

In the photocatalysis mechanism, when light with energy equal to or higher than the band gap energy is incident on a photocatalyst, the energy is absorbed by the electron in the valence band and gets excited to the conduction band, leaving holes, thus creating electron–hole pairs. The generated electrons react with the surrounding oxygen, and the holes react with OH molecules to form superoxide anions (O^{2-}) and hydroxide radicals (OH^-), respectively. These O^{2-} and OH^- further react with dye molecules (organic polutants) decomposing them into CO_2 and H_2O. The following equations summarize the mechanism:

Activation reaction;

$$SnO_2 + hv \rightarrow h^+ + e^- \quad (3)$$

Oxidation reaction;

$$h^+ + OH^- \rightarrow OH^{\cdot} \quad (4)$$

Reduction reaction;

$$e^- + O_2 \rightarrow O_2^{-} \quad (5)$$

$$\text{Organic pollutants} + O_2^{-} \text{ (or } OH^{\cdot}) \rightarrow CO_2 + H_2O \quad (6)$$

The induced photocatalytic degradation of organic pollutants is well known to follow the pseudo first-order kinetic, as indicated by Gajbhiye (2012), which exhibits a linear relationship between $\ln(C_O/C_t)$ and the reaction time, t. (equation 2.1). Figure 9 shows a graph of $\ln(C_O/C_t)$ versus time in minutes for sampled films of the pure SnO_2 and WO_3/SnO_2 (1.5 wt.%) thin films.

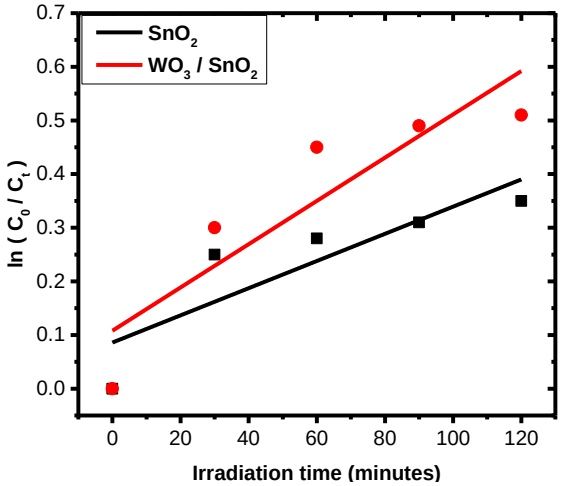

Figure 9: Plot of $\ln(C_O/C_t)$ vs Irradiation time.

The slope of the plot in Figure 9 was used to determine the rate constant, k_c indicated in Figure 10 below which enabled quantification of the photocatalytic activity of the prepared samples. The rate constant determines how fast the degradation takes place. The calculated rate constant values from the above relation (equation 1) are 0.00256 and 0.00519 min^{-1} for SnO_2 and WO_3/SnO_2 (1.5%) films, respectively.

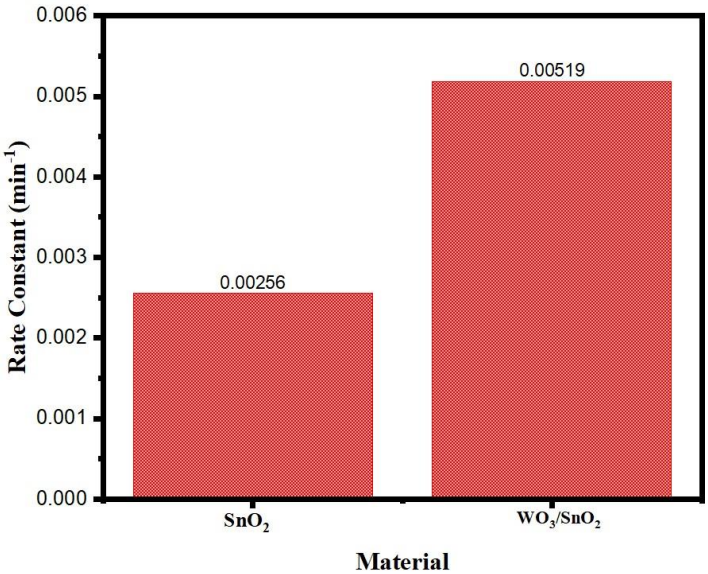

Figure 10: Influence of WO_3 doping on the reaction rate constant.

Based on the results, WO_3/SnO_2 is more efficient in degrading organic pollutants than pure SnO_2, which can be attributed to the following:

(i) Decreased SnO_2 band gap after WO_3 incorporation, from 3.82 to 3.03 eV. This decrease is important in increasing photocatalytic activity (Koohestani 2019) because more electrons are able to gain kinetic energy and move to the conduction band, where they participate in the degradation process.

(ii) Decreased electron-hole pair (EHP) recombination as a result of WO_3 incorporation into the SnO_2 lattice; WO_3 acts as a trap to easily capture the photogenerated electrons and holes on the surface of SnO_2 and thus delay EHP recombination (Manikandan et al. 2018). This is evident in the increased rate constant, showing that the generated electron-hole pairs are contributing to the material's improved photocatalytic performance rather than being lost through recombination.

(iii) Improved light absorption of WO_3/SnO_2 implying that more radiation is absorbed exciting more electrons to the conduction band taking part in the degradation process (Enesca and Sisman 2022). These findings are consistent with those of Ramos-Delgado et al. (2013), who concluded that WO_3/TiO_2 exhibited better photocatalytic behavior than bare TiO_2 due to the formation of smaller clusters and a higher surface area, which reduces electron-hole pair recombination resulting in a better contact area between the catalyst particles and the pollutants (Ramos-Delgado et al. 2013).

Conclusion

Pure SnO_2 and WO_3/SnO_2 thin films were successfully fabricated through the Sol-gel spin coating technique. The influence of the WO_3 doping over the photocatalytic properties of SnO_2 thin films was investigated. Optical analysis revealed that doping SnO_2 thin films with WO_3 leads to a reduction in band gap. The absorbance measurements showed that WO_3/SnO_2 thin films have enhanced absorbance with the peak absorbance shifting towards longer wavelengths. The photocatalytic activity of the deposited films was studied with methylene blue dye under UV irradiation. WO_3/SnO_2 films show superior photocatalytic activity than the undoped SnO_2 films. Therefore, SnO_2 doping with WO_3 is likely to be effective in improving the photocatalytic properties of SnO_2.

Data Availability

The data used to support the findings of this study are included within the article. Further data or information is available from the corresponding author upon request.

Conflicts of Interest

The authors declare that there is no conflict of interest regarding the publication of this article.

Acknowledgements

This work was supported by the International Science Programme (ISP) of Uppsala University, Sweden through Materials Science and Solar Energy Network for Eastern and Southern Africa (MSSEESA) and the Deanship of Scientific Research, Vice Presidency for Graduate Studies and Scientific Research, King Faisal University, Saudi Arabia [Project No. GRAN3000].

ORCIDiDs

Victor Isahi: https://orcid.org/0000-0002-2754-2315

Christopher Maghanga: https://orcid.org/0000-0002-5311-3346

References

Ali T, Tripathi P, Azam A, Raza W, Ahmed AS, Ahmed A and Muneer M 2017 Photocatalytic performance of Fe-doped TiO_2 nanoparticles under visible-light irradiation. *Materials Research Express* 4(1). https://doi.org/10.1088/2053-1591/aa576d

Ameta R and Sharma S 2015 Enhancement of Photocatalytic Activity of Zinc Oxide By Doping with Nitrogen. *Sci. Revs. Chem. Commun*. 5(4): 127–135.

Azim MB, Jani M, Qadir M, Hasanuzzaman M, Gafur M, Gulshan F and Firoz S 2021 *GO*-SnO_2 nanocomposite for photodegradation of methyl orange under direct sunlight irradiation and mechanism insight. Department of Materials and Metallurgical Engineering, BUET, Dhaka, Bangladesh.

Behnajady MA, Modirshahla N and Hamzavi R 2006 Kinetic study on photocatalytic degradation of CI Acid Yellow 23 by ZnO photocatalyst. *J. Hazard. Mater.* 133(1–3): 226–232.

Bhagwat AD, Sawant SS, Ankamwar BG and

Mahajan CM 2015 Synthesis of nanostructured tin oxide (SnO_2) powders and thin films prepared by sol-gel method. *J. Nano- Electron. Phys.* 7(4): 04037.

Buchholz K 2022 *Unsafe Water kills more people than disasters and conflicts*. Statista. https://www.statista.com/chart/17445/global-access-to-safe-drinking-water/

Chatterjee D and Dasgupta S 2005 Visible light induced photocatalytic degradation of organic pollutants. *J. Photochem. Photobiol. C: Photochem. Rev.* 6(2–3): 186–205.

Chaudhary KT 2021 Thin film deposition: Solution based approach. In *Thin Films*. IntechOpen.

Chen P, Liu H, Cui W, Lee SC, Wang L and Dong F 2020 Bi-based photocatalysts for light-driven environmental and energy applications: Structural tuning, reaction mechanisms, and challenges. *EcoMat* 2(3): 1–31.

Doyan A, Hakim S, Muliyadi L and Taufik M 2019 The effect of indium doped SnO_2 thin films on optical properties prepared by Sol-Gel Spin Coating Technique. *J. Phys.: Conf. Ser.* 1397(1): 12005.

Enesca A and Sisman V 2022 Indoor air photocatalytic decontamination by UV–Vis activated $CuS/SnO_2/WO_3$ Heterostructure. *Catalysts* 12(7): 728.

Gajbhiye SB 2012 Photocatalytic degradation study of methylene blue solutions and its application to dye industry effluent. *Int. J. Mod. Eng. Res.* 2(3): 1204–1208.

Han W, Ren L, Qi X, Liu Y, Wei X, Huang Z and Zhong J 2014 Synthesis of CdS/ZnO/graphene composite with high-efficiency photoelectrochemical activities under solar radiation. *Appl. Surface Sci.* 299: 12–18.

Huang T, Qiu Z, Hu Z and Lu X 2021 Novel method of preparing hierarchical porous $CoFe_2O_4$ by the citric acid-assisted sol-gel auto-combustion for supercapacitors. *J. Energ. Storage* 35: 102286.

Iqbal T, Khan MA and Mahmood H 2018 Facile synthesis of ZnO nanosheets: Structural, antibacterial and photocatalytic studies. *Mater. Lett.* 224: 59–63.

Ishchenko O, Rogé V, Lamblin G, Lenoble D and Fechete I 2021 TiO_2, ZnO and SnO_2-based metal oxides for photocatalytic applications: principles and development. *Compt. Rend.. Chim.* 24(1): 103–124.

Islam MJ and Kumer A 2020 First-principles study of structural, electronic and optical properties of $AgSbO_3$ and $AgSb_{0.78}Se_{0.22}O_3$ photocatalyst. *SN Appl. Sci.* 2(2): 251.

Jilani A, Abdel-Wahab MS and Hammad A H 2017 Advance deposition techniques for thin film and coating. *Mod. Technol. Creating Thin-Film Syst. Coat.* https://doi.org/10.5772/65702

Koohestani H 2019 Characterization of TiO_2/WO_3 composite produced with recycled WO_3 nanoparticles from WNiFe alloy. *Mater. Chem. Phys.* 229: 251–256.

Manikandan AS, Renukadevi KB, Ravichandran K and Sindhuja E 2018 Ag activated SnO_2 films for enhanced photocatalytic dye degradation against toxic organic dyes. *J. Mater. Sci.: Mater. Electron.* 29: 8547–8554.

Marikkannan M, Vishnukanthan V, Vijayshankar A, Mayandi J and Pearce J M 2015 A novel synthesis of tin oxide thin films by the sol-gel process for optoelectronic applications. *Aip Advances* 5(2): 27122.

Naseri N, Azimirad R, Akhavan O and Moshfegh AZ 2010 Improved electrochromical properties of sol–gel WO_3 thin films by doping gold nanocrystals. *Thin Solid Films* 518(8): 2250–2257.

Ojha A and Tiwary D 2021 Organic pollutants in water and its health risk assessment through consumption. In *Contamination of Water* (pp. 237–250). Academic Press.

Parashar M, Shukla VK and Singh R 2020 Metal oxides nanoparticles via sol–gel method: a review on synthesis, characterization and applications. *J. Mater. Sci.: Mater. Electron.* 31: 3729–3749.

Raj ILP, Revathy MS, Christy AJ, Chidhambaram N, Ganesh V and AlFaify

S 2020 Study on the synergistic effect of terbium-doped SnO_2 thin film photocatalysts for dye degradation. *J. Nanopart. Res.* 22: 1–14.

Ramos-Delgado NA, Gracia-Pinilla MA, Maya-Trevino L, Hinojosa-Reyes L, Guzman-Mar JL and Hernández-Ramírez A 2013 Solar photocatalytic activity of TiO_2 modified with WO_3 on the degradation of an organophosphorus pesticide. *J. Hazard. Mater.* 263: 36–44.

Rathanasamy R, Kaliyannan GV, Sivaraj S, Muthiah E, Khaan AAA, Ravichandran D and Uddin M 2023 Effect of molybdenum disulphide thin films on enhancing the performance of polycrystalline silicon solar cells. *Int. J. Photoenergy* 2023.

Sönmezoğlu S, Arslan A, Serin T and Serin N 2011 The effects of film thickness on the optical properties of TiO_2–SnO_2 compound thin films. *Phys. Scrip.* 84(6): 65602.

Theiss W 2002 Analysis of optical spectra by computer simulation-from basics to batch mode. *Theiss Hard-Und Software for Optical Spectroscopy: Aachen, Germany.*

Tseng TK, Lin YS, Chen YJ and Chu H 2010 A review of photocatalysts prepared by sol-gel method for VOCs removal. *Int J. Mol. Sci.* 11(6): 2336–2361.

Ubi GM, Ikpeme EV and Essien IS 2022 Essentials of the COVID-19 coronavirus. In *Data Science for COVID-19* (pp. 1–25). Elsevier.

United Nations 2022 *Water and Sanitation*. United Nations Sustainable Development. https://www.un.org/sustainabledevelopment/water-and sanitation

Varghese AR, Amarendra G and Hussain S 2018 Cr: SnO_2 thin films-synthesis and characterization. *AIP Conference Proceedings* 1951(1): 20017.

Wang Y, Sun C, Zhao X, Cui B, Zeng Z, Wang A, Liu G and Cui H 2016 The application of nano-TiO_2 photo semiconductors in agriculture. *Nanoscale Res. Lett.* 11: 1–7.

World Heath Organization 2022 *Drinking-water*. World Health Organization. https://www.who.int/news-room/fact-sheets/detail/drinking-water

Yang L, Wang F, Shu C, Liu P, Zhang W and Hu S 2016 An in-situ synthesis of Ag/AgCl/TiO_2/hierarchical porous magnesian material and its photocatalytic performance. *Sci. Rep.* 6(1): 21617.

Zarei S, Hasheminiasari M, Masoudpanah S M and Javadpour J 2022 Photocatalytic properties of ZnO/SnO_2 nanocomposite films: role of morphology. *J. Mater. Res. Technol.* 17: 2305–2312.

Zhu D and Zhou Q 2019 Action and mechanism of semiconductor photocatalysis on degradation of organic pollutants in water treatment: A review. *Environ. Nanotechnol. Monitor. Manage.* 12: 100255.